Journal of Ethnopharmacology 267 (2021) 113645

Contents lists available at ScienceDirect

Journal of Ethnopharmacology

journal homepage: www.elsevier.com/locate/jethpharm

Methoxyeugenol regulates the p53/p21 pathway and suppresses human endometrial cancer cell proliferation

Bruna Pasqualotto Costa [a,*], Marcella Tornquist Nassr [a], Fernando Mendonça Diz [b], Krist Helen Antunes Fernandes [c], Géssica Luana Antunes [a], Lucas Kich Grun [d], Florencia María Barbé-Tuana [e], Fernanda Bordignon Nunes [a,f], Gisele Branchini [f], Jarbas Rodrigues de Oliveira [a]

[a] Laboratório de Pesquisa em Biofísica Celular e Inflamação, Pontifícia Universidade Católica do Rio Grande do Sul (PUCRS), Porto Alegre, Rio Grande do Sul, Brazil
[b] Programa de Pós-Graduação em Engenharia e Tecnologia de Materiais, Pontifícia Universidade Católica do Rio Grande do Sul (PUCRS), Porto Alegre, Rio Grande do Sul, Brazil
[c] Laboratório de Imunologia Clínica e Experimental, Pontifícia Universidade Católica do Rio Grande do Sul (PUCRS), Porto Alegre, Rio Grande do Sul, Brazil
[d] Programa de Pós-graduação em Pediatria e Saúde da Criança, Pontifícia Universidade Católica do Rio Grande do Sul (PUCRS), Porto Alegre, Rio Grande do Sul, Brazil
[e] Laboratório de Imunobiologia, Pontifícia Universidade Católica do Rio Grande do Sul (PUCRS), Porto Alegre, Rio Grande do Sul, Brazil
[f] Laboratório de Biofísica Celular, Molecular e Computacional, Universidade Federal de Ciências da Saúde de Porto Alegre (UFCSPA), Porto Alegre, Rio Grande do Sul, Brazil

ARTICLE INFO

Keywords:
Methoxyeugenol
Anticancer effect
Reactive oxygen species
p53/p21 pathway
Endometrial cancer

ABSTRACT

Ethnopharmacological relevance: Plant-derived compounds are a reservoir of natural chemicals and can act as drug precursors or prototypes and pharmacological probes. Methoxyeugenol is a natural compound found in plant extracts, such as nutmeg (*Myristica fragrans*), and it presents anthelmintic, antimicrobial, anti-inflammatory activities. Recently, interest in the anticancer activity of plant extracts is increasing and the therapeutic activity of methoxyeugenol against cancer has not yet been explored.

Aim of the study: The present study aimed to evaluate the cancer-suppressive role and the molecular signaling pathways of methoxyeugenol in human endometrial cancer (Ishikawa) cell line.

Materials and methods: Proliferation, viability, and cell toxicity were assessed by direct counting, MTT assay, and LDH enzyme release assay, respectively. Antiproliferative effect were evaluated by nuclear morphological changes along with the cellular mechanisms of apoptosis and senescence by flow cytometry. The underlying molecular and cellular mechanisms were investigated by RT-qPCR, reactive oxygen species (ROS) levels, mitochondrial dysfunction, and proliferative capacity.

Results and conclusions: Methoxyeugenol treatment significantly inhibited the proliferation and viability of Ishikawa cells. Probably triggered by the higher ROS levels and mitochondrial dysfunction, the gene expression of *p53* and *p21* increased and the gene expression of *CDK4/6* decreased in response to the methoxyeugenol treatment. The rise in nuclear size and acidic vesicular organelles corroborate with the initial senescence-inducing signals in Ishikawa cells treated with methoxyeugenol. The antiproliferative effect was not related to cytotoxicity and proved to effectively reduce the proliferative capacity of endometrial cancer cells even after treatment withdrawal. These results demonstrated that methoxyeugenol has a promising anticancer effect against endometrial cancer by rising ROS levels, triggering mitochondrial instability, and modulating cell signaling pathways leading to an inhibition of cell proliferation.

Abbreviations: EC, endometrial cancer; EEC, endometrioid EC; NEEC, non-endometrioid EC; MET, methoxyeugenol; CPPD, cisplatin; LDH, lactate dehydrogenase; RAPA, rapamycin; NMA, nuclear morphometric analysis; AVO, acidic vesicular organelles; ROS, reactive oxygen species; ΔΨm, mitochondrial membrane potential; PCD, programmed cell death; CDKs, cyclin-dependent kinases; CDKIs, cyclin-dependent kinases inhibitors; MAPK, mitogen-activated protein kinase; SA-β-gal, senescence-associated β-galactosidase.

* Corresponding author. Laboratório de Pesquisa em Biofísica Celular e Inflamação, Pontifícia Universidade Católica do Rio Grande do Sul (PUCRS), 6690 Ipiranga Ave., Zip Code: 90610-000, Porto Alegre, RS, Brazil.
E-mail address: brupcosta@gmail.com (B.P. Costa).

https://doi.org/10.1016/j.jep.2020.113645
Received 3 September 2020; Received in revised form 18 November 2020; Accepted 23 November 2020
Available online 30 November 2020

1. Introduction

Cancer is considered the second leading cause of global morbidity and mortality (WHO, 2018). Due to its heterogeneous nature, there is no universal treatment, and the production of high-quality anticancer agents remains extremely challenging (Siddiqui and Rajkumar, 2012).

Endometrial cancer (EC) is the sixth most common type of cancer in the female population (IARC, 2018; Siegel et al., 2019), with over 380, 000 new cases and approximately 90,000 deaths in 2018 (IARC, 2018). Two different types of EC are identified based on tumor histology: endometrioid EC (EEC) and non-endometrioid EC (NEEC). EEC is generally estrogen-dependent and represents 80% of EC cases. In contrast, NEEC develops independently of estrogen (Morice et al., 2016). The worse prognosis is associated with high-grade, recurrent, or metastatic ECCs, although NEEC is clinically more aggressive (Urick and Bell, 2019). Currently, surgical treatment is still the most frequently used in clinical practice. However, depending on the stage of cancer (degree of tumor differentiation), adjuvant radiation and/or chemotherapy may be recommended. Hormonal therapy (progestins, luteinizing hormone-releasing hormone agonists, and aromatase inhibitors) (de Haydu et al., 2016) is an alternative treatment for those patients who wish to preserve fertility or with metastatic disease (Amant et al., 2018). Considering that many patients develop drug resistance and tumor recurrence and the restricted non-hormonal therapeutic options, the search for new therapeutic options is necessary, both for independent use or in combination with pre-established standard therapies (Gehrig and Bae-Jump, 2010).

Chemotherapy is widely used in the treatment of cancer, but its toxic effects are a significant problem. To minimize these effects and seek new therapeutic compounds, several therapies have been proposed and many of them are plant-derived products (Desai et al., 2008). Plants have been used as a form of medicine for thousands of years, as they are a reservoir of natural chemicals, being a potential source of new therapeutic drugs, either in their original or semi-synthetic form (Taneja and Qazi, 2006). Taxanes (paclitaxel and docetaxel) and vinca alkaloids (vincristine and vinblastine) are examples of plant-derived anticancer compounds of clinical significance (Mukhtar et al., 2014).

Methoxyeugenol (4-Allyl-2,6-dimethoxyphenol) is a natural phenolic compound naturally found in spices and herbs, such as nutmeg (*Myristica fragrans*) (López et al., 2015), essential oil of *Myrica esculenta* stem bark (Agnihotri et al., 2012), and essential oil from the root bark of sassafras (*Sassafras albidum*) (Kamdem and Gage, 1995). Although authorized and used as a flavoring in the food industry (EFSA, 2011), the biological activity of methoxyeugenol is mostly unknown. Studies with nutmeg extract, which includes methoxyeugenol in its composition, revealed anthelmintic, antimicrobial, anti-inflammatory, and anticancer activities (Agnihotri et al., 2012; López et al., 2015; Paul et al., 2013; Thuong et al., 2014). Endemic to the Maluku Province of Indonesia, nutmeg is a traditional culinary spice, and the nutmeg oil is used for various medicinal purposes, such as rheumatism, nervousness, vomiting, sprains, headaches, and to alleviate stomach disorders (Van Gils and Cox, 1994). Similarly, the Brazilian red propolis extract, a resinous material gathered from different plants by honeybees (*Apis mellifera* L.), also presents methoxyeugenol in its composition and shows antioxidant, antimicrobial, and anticancer activities (Alencar et al., 2007; Freires et al., 2016; Righi et al., 2011).

Although the anticancer activity of methoxyeugenol has not yet been investigated, other similar natural compounds that belong to the class of phenylpropanoids present antitumor activity (Carvalho et al., 2015). One of these compounds is the eugenol (4-Allyl-2-methoxyphenol), which is found in honey and essential oils of different spices such as clove *(Syzgium aromaticum*) (Pramod et al., 2010). Studies have shown its anticancer properties, preventing tumor progression by modulating apoptosis in both gynecological and non-gynecological cancer cell lines (Abdullah et al., 2018; Al-Sharif et al., 2013; Fathy et al., 2019; Yoo et al., 2005).

Given the therapeutic difficulties in tackling EC and the promising effects of phenylpropanoids, the main objectives of the present study were to test the suppression of methoxyeugenol cell proliferation and its underlying mechanisms against endometrial cancer *in vitro*. The human endometrial adenocarcinoma cell line (Ishikawa) is considered a good model for studying the tumor biology of ECC, which once presents hormone responsiveness (Albitar et al., 2007). For the first time, this study demonstrates the potential anticancer effects of methoxyeugenol through suppression of proliferation regulated by the p53/p21 pathway. These data allow us to identify methoxyeugenol as a molecule with promissory therapeutic effects against endometrial cancer.

2. Materials and methods

2.1. Chemicals and reagents

Human endometrial adenocarcinoma (Ishikawa) cell line was obtained from Rio de Janeiro Cell Bank, BCRJ (Rio de Janeiro, Brazil; code: 0364). African green monkey kidney (VERO) cell line was purchased from American Type Culture Collection, ATCC® (Virginia, EUA; CCL-81™). Dulbecco's modified Eagle's medium (DMEM), fetal bovine serum (FBS), Penicillin-streptomycin (10.000 units/mL) and Trypan blue were procured from Gibco™ (Massachusetts, USA). Methoxyeugenol (4-Allyl-2,6-dimethoxyphenol, #W365505), MTT (3-[4,5-dimethylthiazol-2-yl]-2,5 diphenyl tetrazolium bromide), DPPH (2,2-diphenyl-1-picryl-hydrazyl-hydrate), DCFH-DA (2,7-dichlorofluorescin diacetate), DAPI (4′,6-diamidino-2-phenylindole), Acridine Orange, Gentian violet solution, Tween® 20, Triton™ X-100, and Ascorbic acid were purchased from Sigma-Aldrich (Missouri, USA). Cisplatin (CPPD; Fauldcispla®) was obtained from Libbs Farmacêutica Ltda (São Paulo, Brazil). Lactate dehydrogenase (LDH) kit was purchased from Labtest (Minas Gerais, Brazil) and Anexina V-FITC flow cytometer kit from QuatroG (Porto Alegre, Brazil). Dimethyl Sulfoxide (DMSO) was obtained from Merck (Nova Jersey, EUA). TRIzol™, MitoTracker™ Red CMXRos, and C_{12}FDG (5-Dodecanoylaminofluorescein Di-β-D-Galactopyranoside) were purchased from Invitrogen™ (Massachusetts, USA), GoScript™ Reverse Transcription System kit from Promega (Wisconsin, EUA) and PowerUp™ SYBR™ Green Master Mix kit from Applied Biosystems™ (California, EUA).

2.2. Cell culture and treatment

Ishikawa cells were maintained in fresh DMEM supplemented with 10% FBS and penicillin/streptomycin (100 units/mL). Cells were cultured at 37 °C in a 5% CO_2 humidified incubator. Methoxyeugenol was kept at room temperature and diluted in DMEM with 0.5% DMSO to the required concentrations immediately before use for the treatment of Ishikawa cells. Cells were cultured for 24 h before treatment in all assays. Control wells were divided into (1) *Control*: which received DMEM supplemented with FBS and antibiotics, and (2) *DMSO (0.5%):* which received the vehicle of methoxyeugenol (0.5% DMSO) in addition to the FBS and antibiotics.

Methoxyeugenol (4-Allyl-2,6-dimethoxyphenol; linear formula: $H_2C{=}\ CHCH_2C_6H_2(OCH_3)_2OH$; molecular weight: 194.23) was purchased from Sigma-Aldrich (Cat.#W365505/Lot#STBD5682V), ≥95% FG, method of extraction: FT-NMR spectrometer, PubChem Substance ID: 24901834.

2.3. Cell proliferation

Trypan blue exclusion assay was used to quantitatively evaluate cell proliferation (Strober, 2015). Ishikawa cells were seeded in triplicates at a density of 1×10^4 cells per well in 24-well plates and treated with fresh medium containing different concentrations (30, 60, and 125 μM) of methoxyeugenol. The selected concentrations were based on previous studies that tested the antitumor effects of eugenol against gynecological

cancer cells (Abdullah et al., 2018; Fathy et al., 2019). Cisplatin (CPPD; 10 μM) was used as a positive control (Dąbruś et al., 2020). After 72 h of treatment, cell proliferation was determined by counting cell numbers per well (a mix of 1-part of 0.4% trypan blue and 1-part cell suspension) using a Neubauer hemocytometer and optical microscope (Nikon Optiphot, Japan).

2.4. Cell viability and determination of IC_{50}/IC_{90} values

MTT assay was used to evaluate cell viability by measuring the conversion of MTT into formazan crystal (Meerloo et al., 2011). Ishikawa cells were seeded into 24-well plates (1×10^4 cells per well) and treated as previously described. After 72 h the medium was removed and MTT solution (5 mg/mL) was added and incubated at 37 °C in a CO_2 incubator for 3 h. MTT solution was discarded and formazan crystals were dissolved with DMSO. The optical density (OD) was measured at 570 nm with a reference wavelength of 620 nm in an ELISA microplate reader (EZ Read 400; Biochrom). The concentration of methoxyeugenol required to inhibit cell growth by 50% (IC_{50}) and 90% (IC_{90}) when compared to untreated control cells was determined by plotting the percentage of relative cell viability (%) against the logarithm of the methoxyeugenol concentrations tested to measure the antiproliferative activity.

VERO cells were also studied to verify the effects of the treatment in a non-tumoral cell type. VERO is one of the most common mammalian cells used in research in virology, cellular, and molecular biology, and is also an *in vitro* model for toxicity evaluation of chemical compounds at the molecular level (Ammerman et al., 2008). VERO cells were seeded into 96-well plates (2×10^3 cells per well), treated with methoxyeugenol (30, 60, and 125 μM), and after 72 h MTT assay was performed as described above.

2.5. Cytotoxicity assay

The leakage measurement of lactate dehydrogenase (LDH) enzyme into the cell culture medium was used as a marker of membrane damage, indicative of cytotoxicity. Cells were seeded in triplicates at a density of 1×10^4 cells per well in 24-well plates and treated with fresh medium containing different concentrations (30, 60, and 125 μM) of methoxyeugenol or with CPPD (10 μM). After 72 h, the enzyme activity was measured in both supernatant and cell lysate using the colorimetric assay Lactate dehydrogenase kit according to the manufacturer's instructions. DMEM with 5% Tween®20 solution was used for the cell lysis control. LDH release was calculated by measuring the absorbance at 492 nm using an ELISA microplate reader. Results are expressed as a percent of LDH release in the supernatant.

2.6. Apoptosis assay

Cell death mediated by apoptosis or necrosis was quantified by the double staining assay using Annexin V-FITC and Propidium iodide (PI) flow cytometer kit. Cells were seeded in quadruplicates at a density of 1×10^4 cells per well in 24-well plates and treated with 60 μM of methoxyeugenol or CPPD (10 μM). Methoxyeugenol (60 μM) was chosen based on cell proliferation, viability, and cytotoxicity assays. After 48 h, cells were harvested, washed with ice-cold PBS, re-suspended in binding buffer, and incubated with Annexin V-FITC and PI according to the manufacturer's instructions. Samples were analyzed by FACSCanto II Flow Cytometer (BD, Becton-Dickinson, USA) and data were processed using FlowJo 7.6.5 software (Tree Star Inc., Ashland, OR). The analysis allowed the discrimination between live cells (Annexin V^-/PI^-), early apoptotic cells (Annexin V^+/PI^-), late apoptotic cells (Annexin V^+/PI^+), and necrotic cells (Annexin V^-/PI^+).

2.7. Nuclear morphometric analysis (NMA)

The analysis of the nuclear size and irregularity was performed to investigate the mechanism involved in cell number decrease. Cells were seeded in triplicates at a density of 1×10^4 cells per well in 24-well plates and treated with methoxyeugenol (60 μM) or CPPD (10 μM). After 48 h of treatment, the culture medium was discarded, cells were fixed with 4% paraformaldehyde, and permeabilized with 0.3% Triton™ X-100 in PBS for 30 min. Cells were marked with a fluorescent dye solution of DAPI (300 nM) for 2 min and cell images acquired by an inverted fluorescence microscope. The NMA was performed using Image-Pro Plus 6.0 software (IPP6–Media Cybernetics, Silver Spring, MD). Different nuclear phenotypes were separated in an area versus nuclear irregularity index (NII) plot and control-cell nuclei were used to set the normal parameters (Filippi-Chiela et al., 2012).

2.8. Acidic vesicular organelles quantification

Evidence suggests that the lysosomal content is up-regulated in autophagic (Yim and Mizushima, 2020) and senescent (Lee et al., 2006) cell processes. Acridine orange (AO) is a lysosomotropic dye used to identify acidic vesicular organelles (AVOs). Under the AO staining, the whole cell fluoresces green, whereas the acidic compartments fluoresce orange-red (Paglin et al., 2001). Cells were seeded in triplicates at a density of 1×10^4 cells per well in 24-well plates and treated with methoxyeugenol (60 μM) and Rapamycin (1 ng/mL), a potent inducer of autophagy (Li et al., 2014). After 48 h, cells were harvested and incubated with AO (1 μg/mL) for 15 min at room temperature protected from light. The intensity of fluorescence was quantified by flow cytometry, using the FACSCanto II Flow Cytometer and FlowJo 7.6.5 software. The images of the fluorescent cells were captured by an inverted fluorescence microscope (Eclipse TE2000-S, Nikon).

2.9. mRNA expression analysis

The relative expression of five genes (*p53, p21, p16, CDK4, and CDK6*) involved in the control of cell-cycle progression was evaluated by Real-Time Quantitative Reverse Transcription PCR (RT-qPCR). The activity of the tumor suppressor *p53* is tightly regulated, once it is essential in maintaining cellular genomic integrity and in controlled cell growth (Bargonetti and Manfredi, 2002). While the loss of *p53* function results in the aberrant growth of cells and oncogenic alterations, *p53* activation leads to cell-cycle arrest, senescence, or apoptosis (Brooks and Gu, 2010). Cyclin-dependent kinases (CDKs), such as *CDK4* and *CDK6*, and CDK inhibitors (CKIs), such as *p21* and *p16*, are key regulatory enzymes involved in cell proliferation through regulating cell-cycle checkpoints (Malumbres, 2014).

Cells were seeded in triplicates at a density of 1×10^5 cells per well in 6-well plates and treated with methoxyeugenol (60 μM) or CPPD (10 μM). Total RNA was extracted using TRIzol™ following the manufacturer's protocol, and reverse transcribed into complementary DNA (cDNA) using the GoScript™ Reverse Transcription System kit. The RT-qPCR was performed with the PowerUp™ SYBR™ Green Master Mix kit in StepOne™ Real-Time PCR System (Applied Biosystems, USA). Primer sequences are listed in Table 1. The mean Ct values were used to calculate the relative expression of the target genes normalized by the internal control glyceraldehyde 3-phosphate dehydrogenase (*GAPDH*) using the $2^{-\Delta\Delta Ct}$ formula (Schmittgen and Livak, 2008).

2.10. Senescence-associated β-galactosidase

Senescence was evaluated by senescence-associated β-galactosidase (SA-β-gal) thought C_{12}FDG (5-dodecanoylaminofluorescein di-β-D-galactopyranoside), a fluorogenic substrate for β-galactosidase (Debacq-Chainiaux et al., 2009). Cells were seeded in triplicates at a density of 1×10^4 cells per well in 24-well plates and treated with methoxyeugenol

Table 1
Primer sequences for RT-qPCR.

Genes	Primer sequences (5′-3′)	Product length (bp)
GAPDH	Forward CTT TGT CAA GCT CAT TTC CTG G Reverse TCT TCC TCT TGT GCT CTT GC	133
p53	Forward GTA CCA CCA TCC ACT ACA ACT AC Reverse CAC AAA CAC GCA ACC TCA AAG	142
p21	Forward TGG AGA CTC TCA GGG TCG AAA Reverse GGC GTT GGA GTG GTA GAA ATC	163
p16	Forward CAG TAA CCA TGC CCG CAT AGA Reverse AAG TTT CCC GAG GTT TCT CAG A	92
CDK4	Forward ATG TTG TCC GGC TGA TGG A Reverse CAC CAG GCT TAC CTT GAT CTC CC	68
CDK6	Forward AGA CCC AAG AAG CAG TGT GG Reverse AAG GAG CAA GAG CAT TCA GC	387

(60 μM) or hydrogen peroxide (H_2O_2; 500 μM) as a positive control (Chen and Ames, 1994). After 48 h, cells were harvested, washed once with PBS, and incubated with 100 μM chloroquine for 1 h to induce lysosomal alkalinization. After incubation, cells were supplemented with 33 μM C_{12}FDG and maintained at 37 °C with 5% CO_2. Cells were collected, washed with PBS, and the intensity of fluorescence acquired by flow cytometry in FACSCanto™ II. After hydrolysis by β-galactosidase, C_{12}FDG emits green fluorescence (490/514 nm). Data was expressed by MFI (median fluorescence intensity) of C_{12}FDG fluorescence after analysis in FlowJo 7.0 software.

2.11. Antioxidant activity assay

The antioxidant activity of methoxyeugenol (60 μM) was tested through the DPPH (2,2-diphenyl-1-picryl-hydrazyl-hydrate) assay (Kedare and Singh, 2011). DPPH is characterized as a stable free radical and the assay is based on measuring the antioxidant scavenging capacity based on electron-transfer that produces a violet solution in methanol. In the presence of an antioxidant molecule, the DPPH solution (60 μM) can be reduced, giving rise to a colorless methanol solution. Ascorbic acid (AsA; 550 μg/mL) was used as a positive control. The OD was measured at 515 nm in an ELISA microplate reader.

2.12. Determination of reactive oxygen species (ROS) levels

DCFH-DA assay was performed to determine intracellular ROS levels. The DCFH-DA is a non-fluorescent compound, which becomes fluorescent after oxidation by ROS (Kalyanaraman et al., 2012). Cells were seeded in triplicates at a density of 1×10^4 cells per well in 24-well plates and treated with methoxyeugenol (60 μM) or hydrogen peroxide (H_2O_2; 500 μM) as a positive control (Wang and Roper, 2014). After 48 h, cells were harvested, washed once with PBS, and incubated with DCFH-DA (10 μM) for 30 min at 37 °C. The fluorescence intensity was measured at 485 nm with a reference wavelength of 520 nm in a microplate reader (VICTOR®, PerkinElmer, USA). Data were expressed as fluorescence/10^4 cells.

2.13. Analysis of mitochondrial function

MitoTracker™ Red CMXRos is a fluorescent dye that stains mitochondria in viable cells. Its accumulation is directly dependent upon mitochondrial membrane potential. Cells were seeded in triplicates at a density of 1×10^4 cells per well in 24-well plates and treated with methoxyeugenol (60 μM) or CPPD (10 μM) as a positive control. After 48 h, cells were harvested, washed once with PBS, and incubated with MitoTracker™ Red CMXRos (100 nM) for 30 min at 37 °C protected from the light. The intensity of fluorescence was analyzed by flow cytometry, using the FACSCanto II Flow Cytometer and FlowJo 7.6.5 software.

2.14. Clonogenic cell survival assay

Clonogenic cell survival assay analyzes the ability of a single cell to grow into a colony after removing the action of an external stressor (Franken et al., 2006). Cells were seeded in triplicates at a density of 1×10^4 cells per well in 24-well plates and treated with methoxyeugenol (60 μM) or CPPD (10 μM) as a positive control. After 48 h, viable cells were counted using trypan blue exclusion assay and seeded into 12-well plates (400 cells/well). Cells were cultivated in growth medium DMEM at 37 °C in a humidified atmosphere with 5% CO_2. After 7 days, colonies were washed with PBS and fixed with 4% paraformaldehyde for 20 min. Fixed colonies were stained with a solution of 0.5% gentian violet for 5 min and washed with distilled water. Data were expressed as the number of colonies/well.

2.15. Statistical analysis

The *in vitro* experiments were repeated at least three times, all in triplicate. All results are presented through descriptive statistics (mean ± standard deviation (SD)). One-way analysis of variance (ANOVA) followed by the post-hoc test of Tukey for multiple comparisons was used to compare the means between groups. A significance level was statistically accepted when $p < 0.05$. Statistical analyses were performed using GraphPad Prism 5.0 (GraphPad Software, San Diego, CA).

3. Results

3.1. Effects of methoxyeugenol on the survival of Ishikawa cells

The treatment with methoxyeugenol (MET; Fig. 1A) showed a significant decrease in cell number (Fig. 1B; $p < 0.001$) and cell viability (Fig. 1C; $p < 0.001$) in the two higher concentrations (60 and 125 μM) tested when compared to the control groups (culture medium with and without the DMSO vehicle). Cells treated with MET (30 and 60 μM) did not present significant release levels of LDH (Fig. 1D). However, MET (125 μM) showed a significant increase of LDH into the extracellular medium, evidencing cell membrane disruption (Fig. 1D; $p < 0.05$). No significant difference was found between the control treatment supplemented or not with the vehicle DMSO (0.5%); accordingly, all control group represented graphically from now on refers to the treatment with DMEM supplemented with 0.5% DMSO. Treatment with methoxyeugenol showed a concentration-dependent inhibition of cell proliferation, which resulted in an $IC_{50} = 32.18$ μM and an $IC_{90} = 57.93$ μM (Fig. 1E; $R^2 = 0.9996$). Additionally, the same treatment did not affect the viability of non-tumoral VERO cells (Fig. 1F). MET 60 μM was the selected concentration to continue the experiments, as it reduces cell number and viability without causing cytotoxicity in Ishikawa cells.

3.2. Antiproliferative effects of methoxyeugenol

3.2.1. Methoxyeugenol do not exert a pro-apoptotic effect in Ishikawa cells

Treatment with MET (60 μM) does not reduce the number of viable cells neither increases the number of apoptotic nor necrotic cells (Fig. 2A, 2B, 2C, and 2D; $p > 0.05$). These data suggest that the reduction in cell number and cell viability is not related to the inhibition of proliferation by apoptotic cell death. In accordance with the LDH assay results, the treatment with MET (60 μM) did not induce necrosis, suggesting that this compound is not cytotoxic (Fig. 2D; $p > 0.05$). As expected, the positive control CPPD (10 μM) reduced live cell percentage and increased the other death parameters.

3.2.2. Methoxyeugenol induces changes in nuclear morphology of Ishikawa cells

Several physiological and cell death processes are associated with alterations in nuclear morphology, such as the increase in nuclear size observed in senescent cells in response to chemical or physical stresses

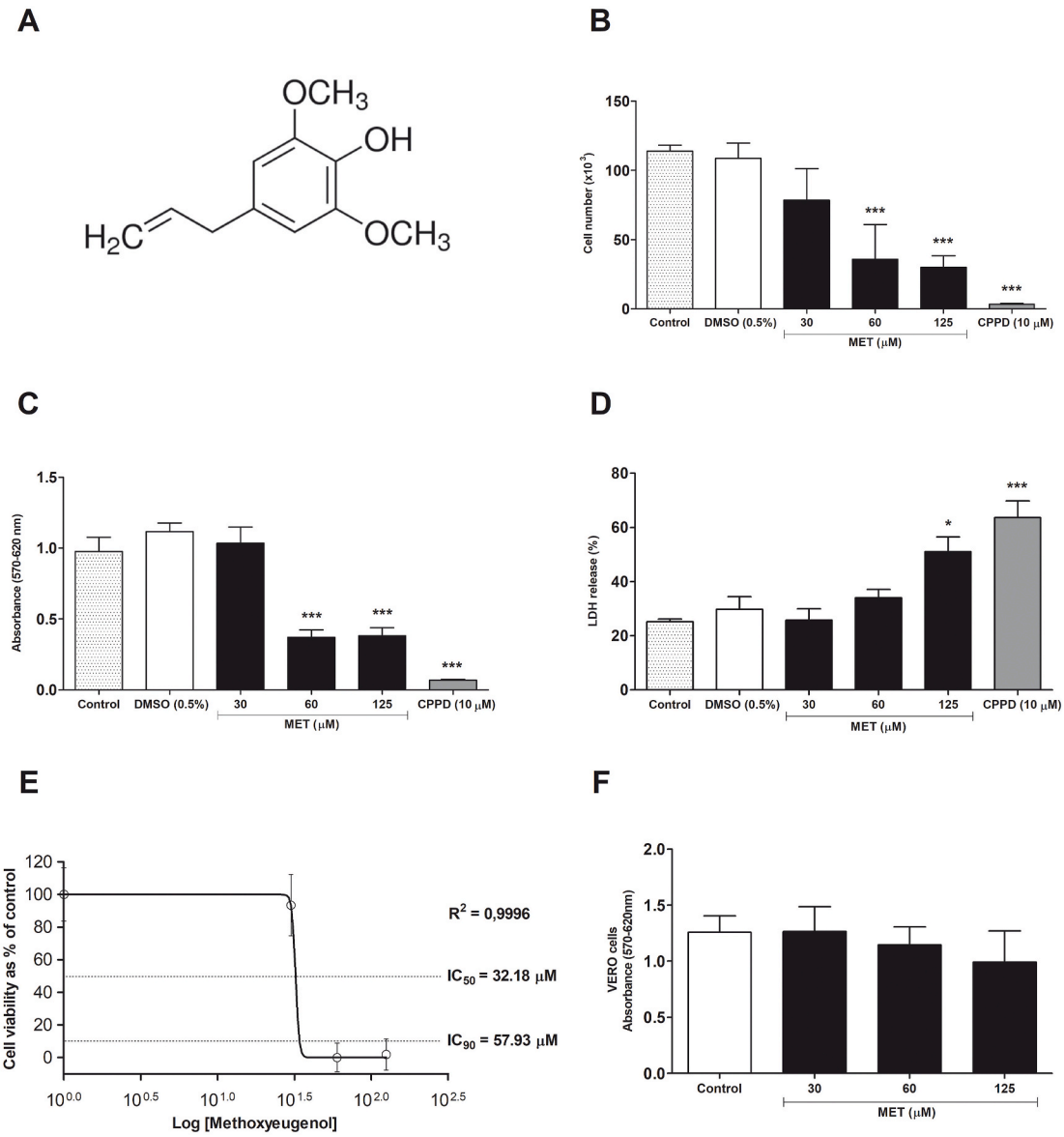

Fig. 1. Effects of methoxyeugenol (MET) in Ishikawa cells after 72 h of treatment. **(A)** Chemical structure of MET. **(B)** Antiproliferative effect of MET on the total cell number count. **(C)** Reduction in cell viability in response to treatment with MET. **(D)** Measurement of LDH enzyme release (cytotoxicity) in response to the MET treatment. Cisplatin (CPPD) was used as a positive control. **(E)** MET-concentrations responsible to inhibit 50% (IC_{50}) and 90% (IC_{90}) of relative cell viability. Control treatment refers to DMEM containing vehicle (0.5% DMSO). **(F)** Effect of MET on the cell viability of non-tumoral VERO cells. Data represent mean ± SD from four (B, C and D) and three (E and F) independent experiments (*$p < 0.05$, ***$p < 0.001$ *vs* control).

(Filippi-Chiela et al., 2012). Fig. 3 shows the percentage of large and regular (LR) nuclei (Fig. 3A), the distribution of size and irregularity nuclei (Fig. 3B), and representative images of nuclei (Fig. 3C) according to the treatment received. As shown in Fig. 3A, there was a rise in the percentage of large and regular nuclei (morphological characteristics associated with the senescence phenotype) in the MET-treated group compared to the control ($p < 0.05$) as well as in the CPPD-treated group ($p < 0.001$). These data suggest that senescence induction is involved in the signaling of MET in Ishikawa cells.

3.2.3. *Methoxyeugenol increases acidic vesicular organelles in Ishikawa cells*

As shown in Fig. 4A, the percentage of acidic compartments (AO-positive cells) increases in response to the treatment with MET (60 μM; $p < 0.05$). Representative flow cytometric plots are shown in Fig. 4B. Fig. 4C displays representative images of AVOs-stained in orange and nuclei and cytoplasm stained in green. As expected, the positive control Rapamycin (RAPA; 1 ng/mL) expressively raises the AVOs. These data suggest that an increase in lysosomal content is one of the cellular responses triggered by the MET in Ishikawa cells.

3.3. *Effects of methoxyeugenol on cell signaling*

3.3.1. *Expression of cell growth regulators in Ishikawa cells*

Cyclins and cyclin-dependent kinases (CDKs) are fundamental regulators of cell-cycle progression through the phosphorylation and inactivation of target substrates. Both *p16* and *p21* families of CDK inhibitors block this phosphorylation and can be under transcriptional control of the *p53* tumor suppressor gene, which is activated by DNA damage (Muñoz-Espín and Serrano, 2014). As shown in Fig. 5A, *p53* expression increase in response to treatments with MET (60 μM; $p < 0.05$) and CPPD (10 μM; $p < 0.001$). There was no difference in the expression levels of *p16* (Fig. 5B; $p > 0.05$) in response to the treatment. MET treatment (60 μM) also raised the expression levels of *p21* (Fig. 5C;

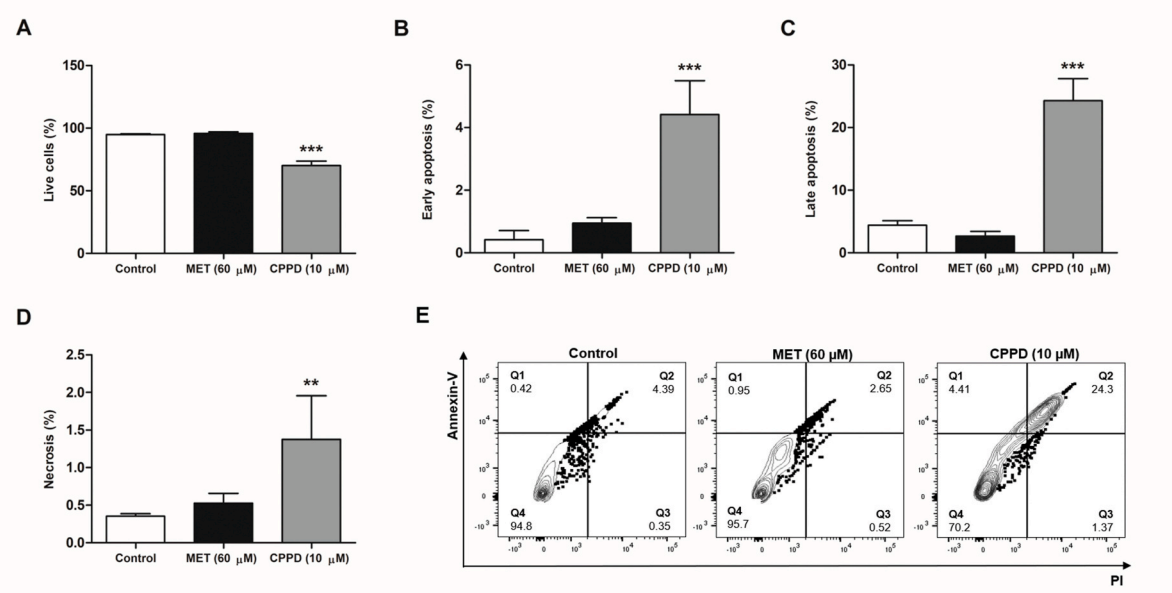

Fig. 2. Effects of methoxyeugenol (MET) on cell death by apoptosis in Ishikawa cells after 48 h of treatment. Results are expressed as a percentage of **(A)** live cells, **(B)** early apoptosis, **(C)** late apoptosis, and **(D)** necrosis. **(E)** Representative flow cytometric plots of control and treatment groups (MET and CPPD). The lower left quadrant (Q4) represents a negative cell cluster (Annexin V^-/PI^-), the upper left quadrant (Q1) shows the cell population positive for one parameter (Annexin V^+/PI^-), the lower right quadrant (Q3) depicts cells positive for the second parameter (Annexin V^-/PI^+), and the upper right quadrant (Q2) represents cells that express both parameters (Annexin V^+/PI^+). A total of 10,000 events were collected and data represent the mean ± SD from four independent experiments (**$p < 0.01$, ***$p < 0.001$ *vs* control).

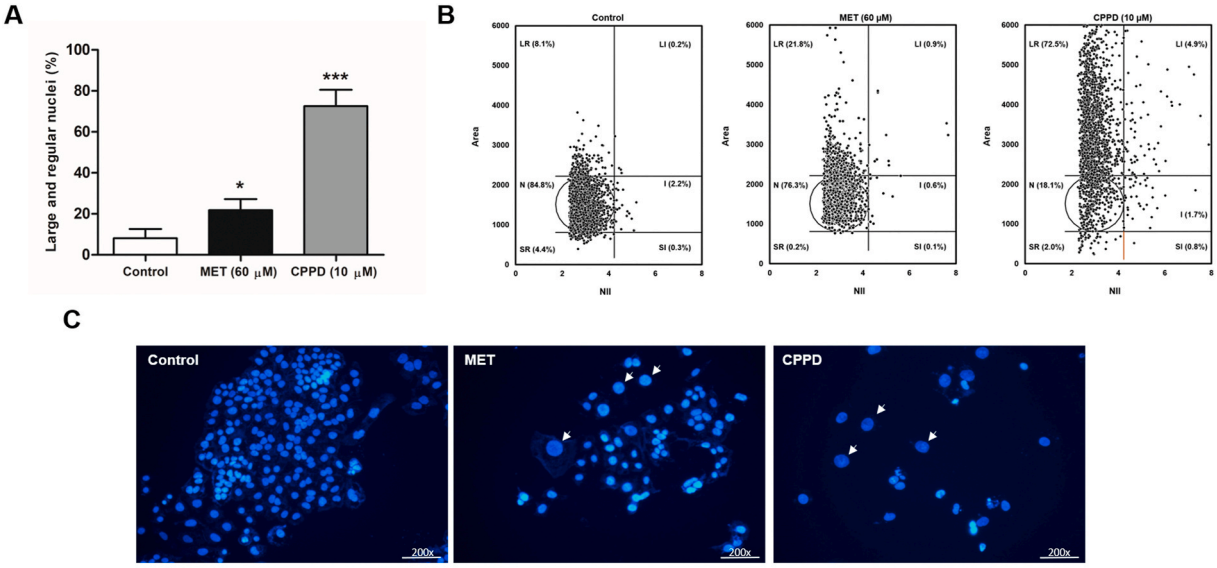

Fig. 3. Effects of methoxyeugenol (MET) on the nuclear morphometry of Ishikawa cells after 48 h of treatment. **(A)** Percentage of large and regular (LR) nuclei (senescence nuclei). **(B)** DAPI-stained nuclei distribution analyses for size and irregularity and the percentages of normal (N), large and regular (LR), small and regular (SR), large and irregular (LI), small and irregular (SI), and irregular (I) nuclei. At least 500 nuclei in three independent experiments were analyzed at each treatment. **(C)** Representative images of DAPI-stained nuclei from control and treated cells (MET and CPPD). White arrows show the large and regular nuclei of senescent cells in MET (60 μM) and CPPD (10 μM) treatment. Data represent the mean ± SD from three independent experiments (*$p < 0.05$, ***$p < 0.001$ *vs* control).

$p < 0.05$) and yet decreased the expression levels of *CDK4* (Fig. 5D; $p < 0.05$). and *CDK6* (Fig. 5E; $p < 0.05$). These results suggest modulation of cell-cycle progression through the *p53-p21* pathway.

3.3.2. *Methoxyeugenol does not increase β-galactosidase activity*

Increased lysosomal activation, indicating by the positive marking for senescence-associated β-galactosidase activity (SA-β-gal), has been used to identify senescent cells (Kurz et al., 2000). According to the median fluorescence intensity (MFI), methoxyeugenol-treated cells did not show an increase in the enzymatic activity of β-galactosidase (Fig. 6A; $p > 0.05$). As expected, the positive control H_2O_2 (500 μM) confirmed the SA-β-gal induction (Fig. 6A; $p < 0.01$). Representative flow cytometric plots are shown in Fig. 6B. These data suggest that there is no fully established senescence state; however, the previous data suggest an antiproliferative effect senescence-mediated in methoxyeugenol-treated Ishikawa cells.

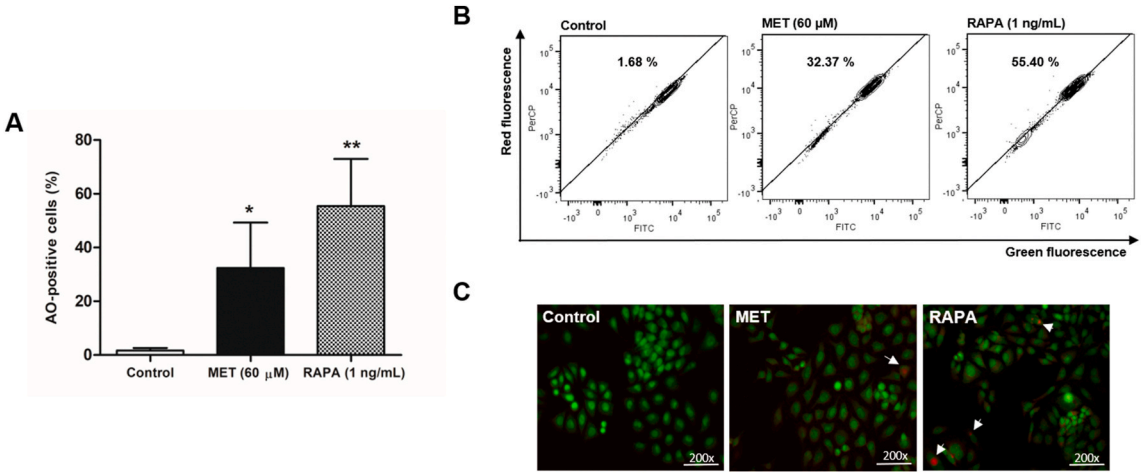

Fig. 4. Effects of methoxyeugenol (MET) in the acidic compartments of Ishikawa cells after 48 h of treatment. **(A)** Percentage of AO-positive cells. **(B)** Representative flow cytometric plots from control and treated cells with MET (60 μM) or Rapamycin (RAPA, 1 ng/mL). A total of 10,000 events were collected and data represent the mean ± SD from three independent experiments (*$p < 0.05$; **$p < 0.01$ *vs* control). **(C)** Representative nuclei images of control and treated cells (MET or RAPA). The white arrows show the acidic vesicular organelles (AVOs) stained in orange. (For interpretation of the references to color in this figure legend, the reader is referred to the Web version of this article.)

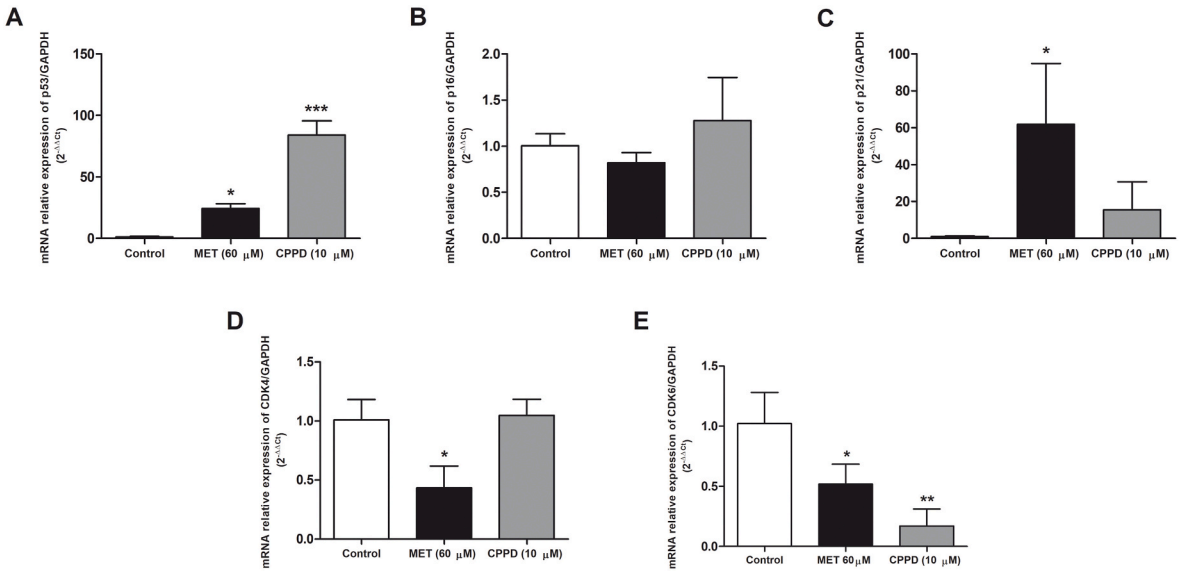

Fig. 5. Effects of methoxyeugenol (MET) on the expression levels of cell growth regulators in Ishikawa cells after 48 h of treatment. Relative mRNA expression of **(A)** *p53*, **(B)** *p16*, **(C)** *p21*, **(D)** *CDK4*, and **(E)** *CDK6* on treatment groups (MET or CPPD). *GAPDH* was used as an internal control. Results are expressed as target gene/GAPDH and data represent the mean ± SD from three independent experiments (*$p < 0.05$, **$p < 0.01$, ***$p < 0.001$ *vs* control).

3.3.3. *Methoxyeugenol induces ROS production in Ishikawa cells*

ROS are by-products of cellular metabolism, however high intracellular levels of ROS can be harmful to cells (Perillo et al., 2020). Despite demonstrating a potent antioxidant effect when analyzed in isolation (Fig. 7A; $p < 0.001$), the intracellular ROS levels significantly grow in response to MET treatment (Fig. 7B; $p < 0.01$) in Ishikawa cells. These results indicate that the increased ROS levels act as intracellular signal molecules directly associated with the triggering of the antiproliferative response of these cells.

3.3.4. *Methoxyeugenol increases mitochondrial membrane potential (ΔΨm)*

A strong positive correlation between ΔΨm and ROS production has been reported (Miwa and Brand, 2003). After 48 h, the Median Fluorescence Intensity (MFI) of MitoTracker™ Red CMXRos (MTR) increased in cells treated with MET (60 μM) (Fig. 8A, $p < 0.01$) or CPPD (10 μM) (Fig. 8A, $p < 0.05$). The percentage of PE-positive cells also higher in treated groups (Fig. 8B). These results indicate a positive relationship between the increase of ROS levels and ΔΨm.

3.4. *Methoxyeugenol reduces the colony-forming capability of Ishikawa cells*

Clonogenic survival assay measures the effects of growth inhibition after the withdrawal of the stimulus/treatment. Cells that received MET (60 μM) as a treatment before the clonogenic survival assays showed a reduced number of colonies (Fig. 9A; $p < 0.01$). The same trend was observed in the CPPD (10 μM) group (Fig. 9A; $p < 0.001$), evidencing that the inhibitory effect on cell proliferation was kept after the removal of these treatments' stimulus.

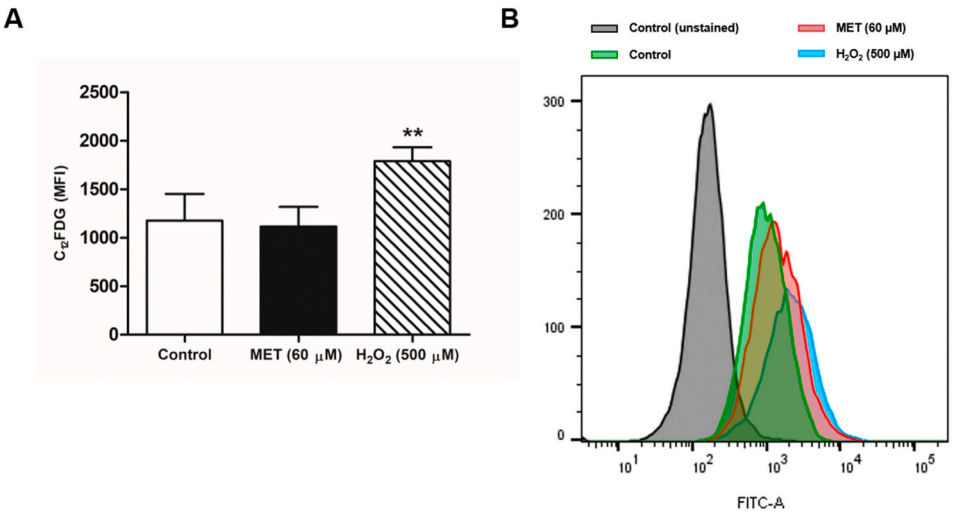

Fig. 6. Effects of methoxyeugenol (MET) on senescence-associated β-galactosidase (SA-β-gal) in Ishikawa cells after 48 h of treatment. **(A)** Median fluorescence intensity (MFI) of fluorochrome C_{12}FDH. H_2O_2 (500 μM) was used as a positive control **(B)** Representative flow cytometric plots of positive cells in control and treated groups (MET and H_2O_2). A total of 10,000 events were collected and data represent the mean ± SD from four independent experiments (**$p < 0.01$ vs control).

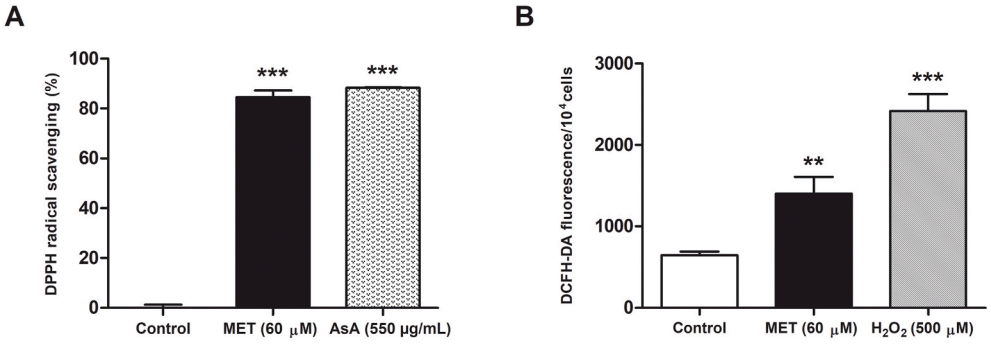

Fig. 7. Methoxyeugenol (MET) antioxidant activity and ROS production in Ishikawa cells after 48 h of treatment. **(A)** Antioxidant activity of the MET (60 μM). Ascorbic acid (AsA, 500 μg/mL) was used as a positive control. Results are presented as a percentage of DPPH reduction. **(B)** Effect of MET (60 μM) on ROS production. H_2O_2 (500 μM) was used as a positive control. Results are expressed as DCFH-DA fluorescence/10^4 cells. Data represent the mean ± SD from three (A) and four (B) independent experiments (**$p < 0.01$, ***$p < 0.001$ *vs* control).

4. Discussion

Clinical use of plant-derived substances with therapeutic properties that can control or interrupt the carcinogenic process provides an important alternative to conventional treatments. The use of plant-derived products has shown to be a promising strategy against cancer, not only as an approach to eliminate tumor cells but also as a molecular modulator of the pathophysiology of cancer (Desai et al., 2008). Methoxyeugenol is one of the compounds found in nutmeg essential oil (*Myristica fragrans*) (López et al., 2015), essential oil of *Myrica esculenta* stem bark (Agnihotri et al., 2012), essential oil from the root bark of *Sassafras albidum* (Kamdem and Gage, 1995), and Brazilian red propolis extract (Alencar et al., 2007; Righi et al., 2011). Studies demonstrate that methoxyeugenol corresponds to approximately 8% of the nutmeg essential oil (López et al., 2015), and 9% of the essential oil of *M. esculenta* stem bark (Agnihotri et al., 2012). Anthelmintic, antimicrobial, anti-inflammatory, and anticancer activities have already been identified in nutmeg extracts, which includes methoxyeugenol in its composition. (Agnihotri et al., 2012; López et al., 2015; Paul et al., 2013; Thuong et al., 2014). The study conducted by Thuong et al. (2014) evaluated antitumor activities of 4 lignans (polyphenols) from the seeds of nutmeg (*Myristica fragrans*). All studied compounds present anticancer properties against various cell lines H1299 (human non-small cell lung carcinoma), H358 (human bronchiolar lung cancer), H460 (large cell lung cancer), HeLa (human cervical cancer), HepG2 (human hepatoblastoma cancer), KPL4 (human breast cancer), and MCF-7, RD (human breast cancer).

Uncontrolled cell proliferation is the main characteristic of tumor progression and the interruption of cell divisions is one of the main targets of anticancer therapies (Pawlowska et al., 2018). In our study, treatment with methoxyeugenol showed an antiproliferative activity and a reduction in the viability of endometrial cancer cells (Ishikawa) when used at 60 and 125 μM. Although the highest concentration of methoxyeugenol (125 μM) caused damage to the cell membrane (cytotoxicity), the reduction in cell number observed at 60 μM does not seem to be related to cell death by necrosis. Even though the approximate concentration of 30 μM of methoxyeugenol is responsible for inhibiting 50% of cell viability (IC_{50}), 60 μM of methoxyeugenol was similar to the IC_{90} value (57.93 μM) demonstrating a promisor anticancer effect against endometrial cancer cells. Also, none of the methoxyeugenol concentrations tested altered the viability of non-tumoral VERO cells. Used as a model to assess the toxicity of chemical compounds at the molecular level, the results found with VERO cells demonstrate a possible selectivity of methoxyeugenol on reducing the viability of tumor cells.

The inability to activate cell elimination mechanisms is involved in the rise of mutations that can lead to carcinogenesis. Thus, cancer treatments aim to stop tumor progression by inducing cell death or stopping cell proliferation pathways. The mechanism of programmed cell death (PCD) is an orderly process and can occur via apoptosis, autophagy, or programmed necrosis, and with the cascade activation of multiple proteins that ultimately lead to cell death (Ouyang et al., 2012). The decrease of cell number in response to treatment with methoxyeugenol proved not to be a consequence of the activation of PCD by

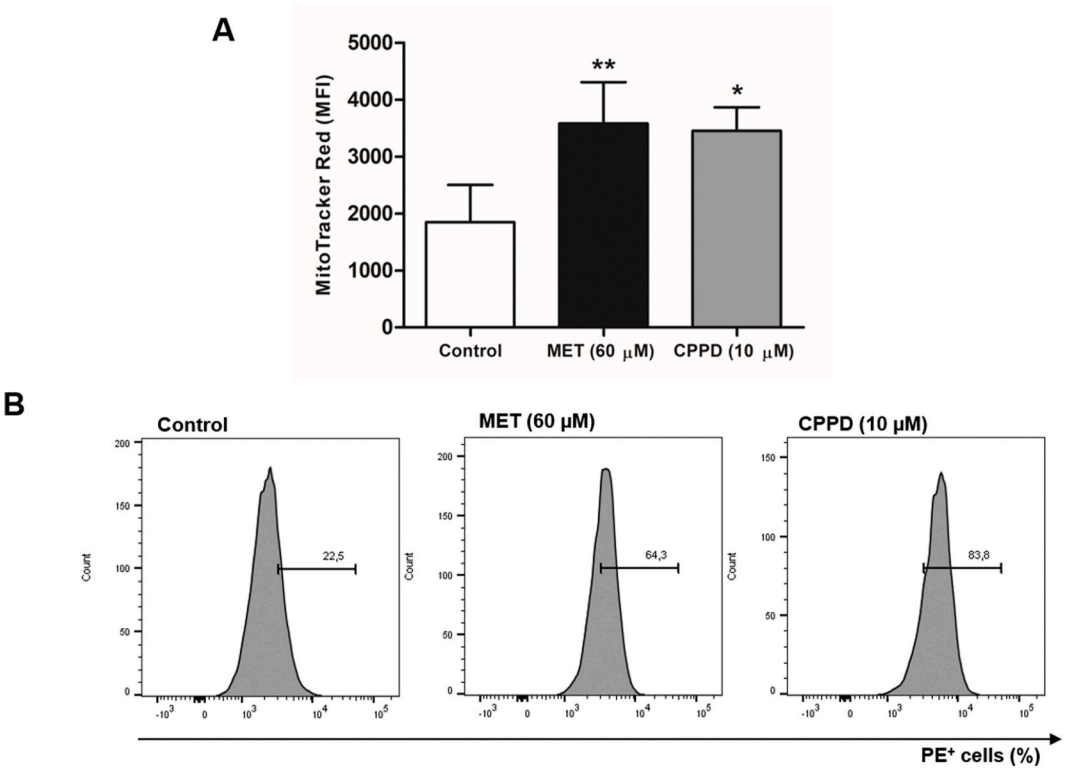

Fig. 8. Effects of methoxyeugenol (MET) on the mitochondrial membrane potential (ΔΨm) of Ishikawa cells after 48 h of treatment. **(A)** Median fluorescence intensity (MFI) of ΔΨm-sensitive fluorochrome MitoTracker™ Red. **(B)** Representative flow cytometric plots of the percentage of PE-positive cells in control and treated groups (MET and CPPD). A total of 10.000 events were collected and data represent the mean ± SD from four independent experiments (*$p < 0.05$, **$p < 0.01$ *vs* control).

apoptosis or necrosis in Ishikawa cells. The non-induction of necrosis corroborates with the results found in the LDH enzyme leakage assay, which proves the non-cytotoxicity of the compound in the concentration used in this study.

A promising approach to contain tumor progression through the regulation of cell proliferation is associated with the permanent interruption of the cell cycle through senescence-induction (Roninson, 2003). Cellular senescence refers to a permanent cell cycle arrest even under cell proliferation signals (Stein et al., 1991). Senescence is often accompanied by phenotypic changes *in vitro*, such as increased cell and nuclei size (Muñoz-Espín and Serrano, 2014), exceptional activation of lysosomes, and positive senescence-associated β-galactosidase activity (Kurz et al., 2000). The accumulation of lysosomal content in senescent cells probably reflects an interesting correlation with autophagy (Young et al., 2009). Combined or exclusive therapies with cisplatin are common and effective practices in antineoplastic treatment. Widely known for generating DNA damage, cisplatin triggers molecular pathways that lead to cell mitosis inhibition and induction of apoptotic cell death, which is directly related to the toxic effects of this chemotherapy in clinical practice (Dasari and Bernard Tchounwou, 2014). Cell senescence-induced by cisplatin has also been reported as one of the mechanisms of action in tumor containment (Li et al., 2014).

Our results demonstrate that methoxyeugenol (60 μM) significantly increases the nuclear size as well as the content of acidic vesicular organelles of Ishikawa cells. Nevertheless, despite being a phenotypic alteration compatible with cellular senescence, the activity of the enzyme β-galactosidase did not increase in response to treatment with methoxyeugenol. Interestingly, Cho et al. (2011) evaluated the kinetics of cellular changes that occur during the progression of senescence induced by DNA damage in the breast cancer cell line MCF-7. In this study, the authors found that cell volume and lysosomal content increased abruptly in the early stages of senescence. Conversely, SA-β-gal increased only after 48 h, suggesting that regulation of β-galactosidase levels requires an induction period in cells that were already in cell cycle arrest (Cho et al., 2011). Considering that in the present study the activity of β-galactosidase was evaluated after 48 h of methoxyeugenol treatment, possibly the low levels of expression of the enzyme were responsible for the low levels of hydrolysis of the fluorescent compound C_{12}FDG. Corroborating with the data found, Uehara et al. (2015) also demonstrated an increase in Ishikawa cell size treated with cisplatin (Uehara et al., 2015).

In normal cells, growth factors (mitogens) are responsible for initiating and maintaining the transition from G1 to S phase in the cell cycle. Mitogen-activated protein kinase (MAPK) signaling pathways stimulate the cell cycle machinery by inducing cyclins, which are the activators of cyclin-dependent kinases (CDKs). Cyclin D1 activates CDKs (such as CDK4 or CDK6) and phosphorylates the retinoblastoma protein (pRb) thereby stimulating downstream cell cycle machinery. CDKs can be blocked, directly or through the induction of CDK inhibitors (CDKIs) leading to cell growth arrest (Lim and Kaldis, 2013). The senescence program is driven by a complex interplay of signaling pathways that converge on the activation of cell cycle inhibitors (Muñoz-Espín and Serrano, 2014). The molecular characteristics of senescent cells usually include upregulation of CDKIs such as p21 and/or p16 (He et al., 2017). Once p53 is activated, it increases the expression of p21, which interacts and inhibits the activity of the cyclin-CDK2, -CDK1 and -CDK4/6 complexes, regulating the cell cycle progression during the G1 and S phases (Gartel and Radhakrishnan, 2005), thereby preventing phosphorylation of pRb and suppressing the expression of proliferation-associated genes (Narita et al., 2003). Our results showed an upregulation in *p53* and *p21* gene expression, and a downregulation in *CDK4* and *CDK6* gene expression in response to treatment with methoxyeugenol. These results showed a strong correlation between the reduction in the cell number and the induction of G1/S-phase cell cycle arrest, triggered by the

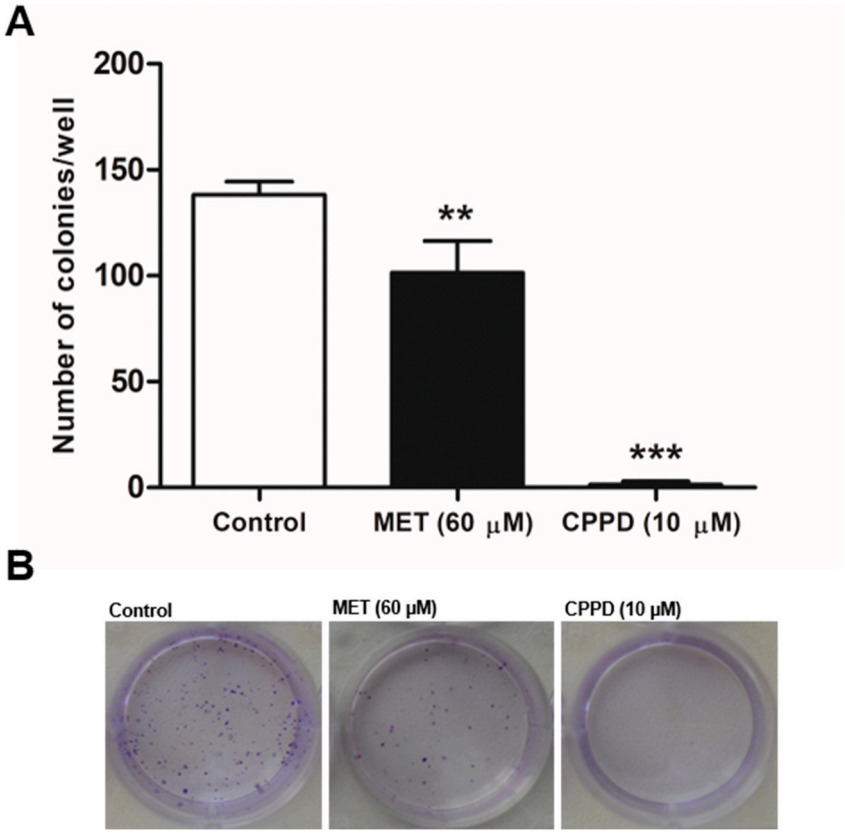

Fig. 9. Effects of methoxyeugenol (MET) on the colony-forming capability of Ishikawa cells. After 48 h of treatment, cells were harvested, seeded (400 cells/well), and incubated for 7 days. **(A)** The total number of colonies per well. **(B)** Representative images of colonies from control and treated cells with MET (60 μM) or CPPD (10 μM). Data represent the mean ± SD from three independent experiments (**$p < 0.01$, ***$p < 0.001$ *vs* control).

p53-p21 pathway, which is an important regulator of the progression of cell senescence. Cho et al. (2011) also identified a rapid increase in p53 and p21 levels in the early stages of senescence in MCF-7 cells (Cho et al., 2011). Methoxyeugenol did not affect *p16* gene expression levels.

Cellular senescence can be triggered in response to multiple stressors and damaging agents, including telomere shortening, DNA damage, oncogenic signaling, and ROS (Muñoz-Espín and Serrano, 2014). Although moderate levels of ROS contribute to the control of cell proliferation and differentiation (Perillo et al., 2020), high levels of ROS that exceed cellular antioxidant capacity lead to oxidative stress, severely damaging biomolecules such as DNA, proteins, and lipids (Ježek and Hlavatá, 2005). ROS levels increase after several different types of stress, such as chemotherapeutic agents and DNA damage, and can trigger programmed cell death (Azad et al., 2009). Interestingly, a rise in ROS levels can also promote cellular senescence through the activation of $p38^{MAPK}$, leading to the increased transcriptional activity of *p53* and upregulation of *p21* (Debacq-Chainiaux et al., 2010). Our results showed that Ishikawa cells treated with methoxyeugenol increased ROS levels. These data highlight the role of ROS modulation as a key factor in signaling anticancer treatment pathways.

Natural phenolic compounds, such as phenylpropanoids, are part of the diet and have health-beneficial properties, largely due to their high antioxidant capacity (Zhang et al., 2015). Although antioxidant treatment has been reported to delay or prevent cell senescence (Lee et al., 1999), methoxyeugenol showed high antioxidant activity; in contrast, when in cell culture, methoxyeugenol demonstrated to act in a pro-oxidant way, increasing the levels of intracellular ROS. Nevertheless, studies conducted with eugenol, a compound of the phenylpropanoid class, same class as methoxyeugenol, demonstrated a double effect on oxidative stress: (1) cancer-preventive action due to its effective antioxidant nature and (2) pro-oxidant action that affects several cell signaling pathways, culminating in the death of tumor cells (Bezerra et al., 2017).

Interestingly, antioxidant compounds can also exert pro-oxidant activities under certain conditions, such as in the presence of metal ions and when administered in high doses (Raza and John, 2005; Sotler et al., 2019). Due to redox cycling capacity, iron and copper are essential for many biological functions because they act as cofactors and cell mediators (Cai et al., 2005; Kalinowski and Richardson, 2005). However, under redox cycling reactions, these metallic ions also result in cytotoxicity through the donation of electrons to oxygen, leading to the generation of ROS, such as superoxide and hydroxyl radicals (Jomova and Valko, 2011). Thus, the concentration of redox-active metal ions is tightly regulated in mammalian cells allowing their bioavailability but also avoiding the generation of ROS (Grubman and White, 2014; Lane et al., 2015). Consequently, imbalances in the concentrations of redox cycling metals are frequently observed in several pathologies, including cancer (Kalinowski et al., 2016). High levels of copper have been found in gynecological tumors of the breast, cervix, and ovaries (Gupte and Mumper, 2009). Antitumor therapies have already been proposed to act on the redox cycling of metal by depleting iron or copper or by generating cytotoxic ROS levels in cancer cells (Kalinowski et al., 2016; Torti and Torti, 2013). The mobilization of endogenous copper ions in humans by the pro-oxidant activity of phenolic compounds can lead to oxidative DNA damage and be responsible for inducing antitumor properties (Azmi et al., 2006; Farhan et al., 2016; Galati and O'Brien, 2004).

Although not fully understood, the production of ROS by mitochondria seems to be influenced by the ΔΨm, consequently affecting several cellular processes, such as the control of redox and pH microenvironment, which can ultimately affect mechanisms of cell proliferation and death (Zorova et al., 2018). The ΔΨm can have a paradoxical

effect. While low ΔΨm values are related to insufficient ATP production, low ROS levels, and cell death (Perillo et al., 2020), the mitochondrial respiratory chain becomes a significant producer of ROS in response to a high ΔΨm (Starkov and Fiskum, 2003). Cisplatin, a chemotherapeutic drug known to induce DNA damage leading to cell death, has been shown to mediate its effects by increasing ROS and ΔΨm in ovarian cancer cells (Kleih et al., 2019). Therefore, mitochondrial hyperpolarization can lead to an exponential increase in the generation of ROS, and maintaining an excessively high ΔΨm can lead to mitochondrial and cellular damage (Gergely et al., 2002). Interestingly, in addition to the rise in ROS levels, the ΔΨm of Ishikawa cells also increase in response to treatment with methoxyeugenol, leading to cell damages.

5. Conclusion

Medicinal plants have been considered a valuable source of compounds with pharmacological activities. Here we demonstrate that methoxyeugenol (60 μM) was able to increase ROS levels and induce mitochondrial damage in Ishikawa cells. The high ROS levels show to be responsible for the activation of antiproliferative signaling pathways. Methoxyeugenol upregulates the expression of *p53* and *p21*, which in turn inhibits *CDK4/6* and triggers the inhibition of cell cycle progression. Cell phenotypic changes such as enlarged nuclear size and the increased number of acidic vesicular organelles corroborate with the initial senescence-inducing phenotype in Ishikawa cells treated with methoxyeugenol. The antiproliferative effect did not cause cytotoxicity and proved to be effective in reducing the proliferative capacity of endometrial cancer cells even after treatment withdrawal. Our findings uncovered the promising anticancer effect of methoxyeugenol in endometrial cancer cells and which molecular mechanisms are involved in this therapeutic response.

Credit author statement

BPC: Conceptualization, Methodology, Investigation, Formal analysis, Validation, Writing, Review & Editing; **MTN, FMD, KHAF, GLA, LKG,** and **FMBT:** Investigation, Formal analysis, Validation; **FBN:** Project administration, Review & Editing; **GB:** Methodology, Formal analysis, Validation, Review & Editing; and **JRO:** Methodology, Formal analysis, Validation, Resources, Review & Editing.

Funding

This study was financed in part by the Coordenação de Aperfeiçoamento de Pessoal de Nível Superior – Brasil (CAPES) – Finance Code 001.

Ethical approval

This article does not contain any studies with human participants or animals, performed by any of the authors.

Declaration of competing interest

The authors do not have any conflict of interest.

Acknowledgements

We thank Fernanda Teixeira Subtil, MSc (The Francis Crick Institute) for intellectual assistance and proofreading the manuscript.

References

Abdullah, M.L., Hafez, M.M., Al-Hoshani, A., Al-Shabanah, O., 2018. Anti-metastatic and anti-proliferative activity of eugenol against triple negative and HER2 positive breast cancer cells. BMC Compl. Alternative Med. 18, 321. https://doi.org/10.1186/s12906-018-2392-5.

Agnihotri, S., Wakode, S., Ali, M., 2012. Essential oil of Myrica esculenta Buch. Ham.: composition, antimicrobial and topical anti-inflammatory activities. Nat. Prod. Res. 26, 2266–2269. https://doi.org/10.1080/14786419.2011.652959.

Al-Sharif, I., Remmal, A., Aboussekhra, A., 2013. Eugenol triggers apoptosis in breast cancer cells through E2F1/survivin down-regulation. BMC Canc. 13, 600. https://doi.org/10.1186/1471-2407-13-600.

Albitar, L., Pickett, G., Morgan, M., Davies, S., Leslie, K.K., 2007. Models representing type I and type II human endometrial cancers: Ishikawa H and Hec50co cells. Gynecol. Oncol. 106, 52–64. https://doi.org/10.1016/j.ygyno.2007.02.033.

Alencar, S.M., Oldoni, T.L.C., Castro, M.L., Cabral, I.S.R., Costa-Neto, C.M., Cury, J.A., Rosalen, P.L., Ikegaki, M., 2007. Chemical composition and biological activity of a new type of Brazilian propolis: red propolis. J. Ethnopharmacol. 113, 278–283. https://doi.org/10.1016/j.jep.2007.06.005.

Amant, F., Mirza, M.R., Koskas, M., Creutzberg, C.L., 2018. Cancer of the corpus uteri. Int. J. Gynecol. Obstet. 143, 37–50. https://doi.org/10.1002/ijgo.12612.

Ammerman, N.C., Beier-Sexton, M., Azad, A.F., 2008. Growth and maintenance of vero cell lines. Curr. Protoc. Microbiol. 11 https://doi.org/10.1002/9780471729259.mca04es11.

Azad, M.B., Chen, Y., Gibson, S.B., 2009. Regulation of autophagy by reactive oxygen species (ROS): implications for cancer progression and treatment. Antioxidants Redox Signal. 11, 777–790. https://doi.org/10.1089/ars.2008.2270.

Azmi, A.S., Bhat, S.H., Hanif, S., Hadi, S.M., 2006. Plant polyphenols mobilize endogenous copper in human peripheral lymphocytes leading to oxidative DNA breakage: a putative mechanism for anticancer properties. FEBS Lett. 580, 533–538. https://doi.org/10.1016/j.febslet.2005.12.059.

Bargonetti, J., Manfredi, J.J., 2002. Multiple roles of the tumor suppressor p53. Curr. Opin. Oncol. 14, 86–91. https://doi.org/10.1097/00001622-200201000-00015.

Bezerra, D., Militão, G., de Morais, M., de Sousa, D., 2017. The dual antioxidant/prooxidant effect of eugenol and its action in cancer development and treatment. Nutrients 9, 1367. https://doi.org/10.3390/nu9121367.

Brooks, C.L., Gu, W., 2010. New insights into p53 activation. Cell Res. 20, 614–621. https://doi.org/10.1038/cr.2010.53.

Cai, L., Li, X.-K., Song, Y., Cherian, M., 2005. Essentiality, toxicology and chelation therapy of zinc and copper. Curr. Med. Chem. 12, 2753–2763. https://doi.org/10.2174/092986705774462950.

Carvalho, A.A., Andrade, L.N., de Sousa, É.B.V., de Sousa, D.P., 2015. Antitumor phenylpropanoids found in essential oils. BioMed Res. Int. 1–21. https://doi.org/10.1155/2015/392674.

Chen, Q., Ames, B.N., 1994. Senescence-like growth arrest induced by hydrogen peroxide in human diploid fibroblast F65 cells. Proc. Natl. Acad. Sci. Unit. States Am. 91, 4130–4134. https://doi.org/10.1073/pnas.91.10.4130.

Cho, S., Park, J., Hwang, E.S., 2011. Kinetics of the cell biological changes occurring in the progression of DNA damage-induced senescence. Mol. Cell. 31, 539–546. https://doi.org/10.1007/s10059-011-1032-4.

Dąbruś, D., Kiełbasiński, R., Grabarek, B.O., Boroń, D., 2020. Evaluation of the impact of cisplatin on variances in the expression pattern of leptin-related genes in endometrial cancer cells. Int. J. Mol. Sci. 21, 4135. https://doi.org/10.3390/ijms21114135.

Dasari, S., Bernard Tchounwou, P., 2014. Cisplatin in cancer therapy: molecular mechanisms of action. Eur. J. Pharmacol. 740, 364–378. https://doi.org/10.1016/j.ejphar.2014.07.025.

de Haydu, C., Black, J.D., Schwab, C.L., English, D.P., Santin, A.D., 2016. An update on the current pharmacotherapy for endometrial cancer. Expet Opin. Pharmacother. 17, 489–499. https://doi.org/10.1517/14656566.2016.1127351.

Debacq-Chainiaux, F., Boilan, E., Le Moutier, J.D., Weemaels, G., Toussaint, O., 2010. p38MAPK in the senescence of human and murine fibroblasts. Advances in Experimental Medicine and Biology, pp. 126–137. https://doi.org/10.1007/978-1-4419-7002-2_10.

Debacq-Chainiaux, F., Erusalimsky, J.D., Campisi, J., Toussaint, O., 2009. Protocols to detect senescence-associated beta-galactosidase (SA-βgal) activity, a biomarker of senescent cells in culture and in vivo. Nat. Protoc. 4, 1798–1806. https://doi.org/10.1038/nprot.2009.191.

Desai, A., Qazi, G., Ganju, R., El-Tamer, M., Singh, J., Saxena, A., Bedi, Y., Taneja, S., Bhat, H., 2008. Medicinal plants and cancer chemoprevention. Curr. Drug Metabol. 9, 581–591. https://doi.org/10.2174/138920008785821657.

EFSA, 2011. Scientific Opinion on the safety and efficacy of allylhydroxybenzenes (chemical group 18) when used as flavourings for all animal species. EFSA J 9, 2440. https://doi.org/10.2903/j.efsa.2011.2440.

Farhan, M., Oves, M., Chibber, S., Hadi, S., Ahmad, A., 2016. Mobilization of nuclear copper by green tea polyphenol epicatechin-3-gallate and subsequent prooxidant breakage of cellular DNA: implications for cancer chemotherapy. Int. J. Mol. Sci. 18, 34. https://doi.org/10.3390/ijms18010034.

Fathy, M., Fawzy, M.A., Hintzsche, H., Nikaido, T., Dandekar, T., Othman, E.M., 2019. Eugenol exerts apoptotic effect and modulates the sensitivity of HeLa cells to cisplatin and radiation. Molecules 24, 3979. https://doi.org/10.3390/molecules24213979.

Filippi-Chiela, E.C., Oliveira, M.M., Jurkovski, B., Callegari-Jacques, S.M., Silva, V.D. da, Lenz, G., 2012. Nuclear morphometric analysis (NMA): screening of senescence, apoptosis and nuclear irregularities. PLoS One 7, e42522. https://doi.org/10.1371/journal.pone.0042522.

Franken, N.A.P., Rodermond, H.M., Stap, J., Haveman, J., van Bree, C., 2006. Clonogenic assay of cells in vitro. Nat. Protoc. 1, 2315–2319. https://doi.org/10.1038/nprot.2006.339.

Freires, I.A., de Alencar, S.M., Rosalen, P.L., 2016. A pharmacological perspective on the use of Brazilian Red Propolis and its isolated compounds against human diseases. Eur. J. Med. Chem. 110, 267–279. https://doi.org/10.1016/j.ejmech.2016.01.033.

Galati, G., O'Brien, P.J., 2004. Potential toxicity of flavonoids and other dietary phenolics: significance for their chemopreventive and anticancer properties. Free Radic. Biol. Med. 37, 287–303. https://doi.org/10.1016/j.freeradbiomed.2004.04.034.

Gartel, A.L., Radhakrishnan, S.K., 2005. Lost in transcription: p21 repression, mechanisms, and consequences: Figure-1. Canc. Res. 65, 3980–3985. https://doi.org/10.1158/0008-5472.CAN-04-3995.

Gehrig, P.A., Bae-Jump, V.L., 2010. Promising novel therapies for the treatment of endometrial cancer. Gynecol. Oncol. 116, 187–194. https://doi.org/10.1016/j.ygyno.2009.10.041.

Gergely, P., Niland, B., Gonchoroff, N., Pullmann, R., Phillips, P.E., Perl, A., 2002. Persistent mitochondrial hyperpolarization, increased reactive oxygen intermediate production, and cytoplasmic alkalinization characterize altered IL-10 signaling in patients with systemic lupus erythematosus. J. Immunol. 169, 1092–1101. https://doi.org/10.4049/jimmunol.169.2.1092.

Grubman, A., White, A.R., 2014. Copper as a key regulator of cell signalling pathways. Expet Rev. Mol. Med. 16, e11. https://doi.org/10.1017/erm.2014.11.

Gupte, A., Mumper, R.J., 2009. Elevated copper and oxidative stress in cancer cells as a target for cancer treatment. Canc. Treat Rev. 35, 32–46. https://doi.org/10.1016/j.ctrv.2008.07.004.

He, L., Chen, Y., Feng, J., Sun, W., Li, S., Ou, M., Tang, L., 2017. Cellular senescence regulated by SWI/SNF complex subunits through p53/p21 and p16/pRB pathway. Int. J. Biochem. Cell Biol. 90, 29–37. https://doi.org/10.1016/j.biocel.2017.07.007.

IARC, 2018. World Health Organization International Agency for Research on Cancer (IARC) - Global Cancer Observatory (GLOBOCAN) [WWW Document]. World Heal. Organ. URL. http://globocan.iarc.fr/Pages/fact_sheets_cancer.aspx.

Ježek, P., Hlavatá, L., 2005. Mitochondria in homeostasis of reactive oxygen species in cell, tissues, and organism. Int. J. Biochem. Cell Biol. 37, 2478–2503. https://doi.org/10.1016/j.biocel.2005.05.013.

Jomova, K., Valko, M., 2011. Advances in metal-induced oxidative stress and human disease. Toxicology 283, 65–87. https://doi.org/10.1016/j.tox.2011.03.001.

Kalinowski, D.S., Richardson, D.R., 2005. The evolution of iron chelators for the treatment of iron overload disease and cancer. Pharmacol. Rev. 57, 547–583. https://doi.org/10.1124/pr.57.4.2.

Kalinowski, D.S., Stefani, C., Toyokuni, S., Ganz, T., Anderson, G.J., Subramaniam, N.V., Trinder, D., Olynyk, J.K., Chua, A., Jansson, P.J., Sahni, S., Lane, D.J.R., Merlot, A. M., Kovacevic, Z., Huang, M.L.H., Lee, C.S., Richardson, D.R., 2016. Redox cycling metals: pedaling their roles in metabolism and their use in the development of novel therapeutics. Biochim. Biophys. Acta Mol. Cell Res. 1863, 727–748. https://doi.org/10.1016/j.bbamcr.2016.01.026.

Kalyanaraman, B., Darley-Usmar, V., Davies, K.J.A., Dennery, P.A., Forman, H.J., Grisham, M.B., Mann, G.E., Moore, K., Roberts, L.J., Ischiropoulos, H., 2012. Measuring reactive oxygen and nitrogen species with fluorescent probes: challenges and limitations. Free Radic. Biol. Med. 52, 1–6. https://doi.org/10.1016/j.freeradbiomed.2011.09.030.

Kamdem, D., Gage, D., 1995. Chemical composition of essential oil from the root bark of sassafras albidum. Planta Med. 61, 574–575. https://doi.org/10.1055/s-2006-959379.

Kedare, S.B., Singh, R.P., 2011. Genesis and development of DPPH method of antioxidant assay. J. Food Sci. Technol. 48, 412–422. https://doi.org/10.1007/s13197-011-0251-1.

Kleih, M., Böpple, K., Dong, M., Gaißler, A., Heine, S., Olayioye, M.A., Aulitzky, W.E., Essmann, F., 2019. Direct impact of cisplatin on mitochondria induces ROS production that dictates cell fate of ovarian cancer cells. Cell Death Dis. 10, 851. https://doi.org/10.1038/s41419-019-2081-4.

Kurz, D.J., Decary, S., Hong, Y., Erusalimsky, J.D., 2000. Senescence-associated (beta)-galactosidase reflects an increase in lysosomal mass during replicative ageing of human endothelial cells. J. Cell Sci. 113 (Pt 2), 3613–3622.

Lane, D.J.R., Merlot, A.M., Huang, M.L.-H., Bae, D.-H., Jansson, P.J., Sahni, S., Kalinowski, D.S., Richardson, D.R., 2015. Cellular iron uptake, trafficking and metabolism: key molecules and mechanisms and their roles in disease. Biochim. Biophys. Acta Mol. Cell Res. 1853, 1130–1144. https://doi.org/10.1016/j.bbamcr.2015.01.021.

Lee, A.C., Fenster, B.E., Ito, H., Takeda, K., Bae, N.S., Hirai, T., Yu, Z.-X., Ferrans, V.J., Howard, B.H., Finkel, T., 1999. Ras proteins induce senescence by altering the intracellular levels of reactive oxygen species. J. Biol. Chem. 274, 7936–7940. https://doi.org/10.1074/jbc.274.12.7936.

Lee, B.Y., Han, J.A., Im, J.S., Morrone, A., Johung, K., Goodwin, E.C., Kleijer, W.J., DiMaio, D., Hwang, E.S., 2006. Senescence-associated β-galactosidase is lysosomal β-galactosidase. Aging Cell 5, 187–195. https://doi.org/10.1111/j.1474-9726.2006.00199.x.

Li, J., Kim, S.G., Blenis, J., 2014. Rapamycin: one drug, many effects. Cell Metabol. 19, 373–379. https://doi.org/10.1016/j.cmet.2014.01.001.

Li, W., Wang, W., Dong, H., Li, Y., Li, L., Han, L., Han, Z., Wang, S., Ma, D., Wang, H., 2014. Cisplatin-induced senescence in ovarian cancer cells is mediated by GRP78. Oncol. Rep. 31, 2525–2534. https://doi.org/10.3892/or.2014.3147.

Lim, S., Kaldis, P., 2013. Cdks, cyclins and CKIs: roles beyond cell cycle regulation. Development 140, 3079–3093. https://doi.org/10.1242/dev.091744.

López, V., Gerique, J., Langa, E., Berzosa, C., Valero, M.S., Gómez-Rincón, C., 2015. Antihelmintic effects of nutmeg (Myristica fragans) on Anisakis simplex L3 larvae obtained from Micromesistius potassou. Res. Vet. Sci. 100, 148–152. https://doi.org/10.1016/j.rvsc.2015.03.033.

Malumbres, M., 2014. Cyclin-dependent kinases. Genome Biol. 15, 122. https://doi.org/10.1186/gb4184.

Meerloo, J. Van, Kaspers, G.J.L., Cloos, J., 2011. Cell sensitivity assays: the MTT assay. Cancer cell cult. Methods Mol. Biol. 731, 237–245. https://doi.org/10.1007/978-1-61779-080-5.

Miwa, S., Brand, M.D., 2003. Mitochondrial matrix reactive oxygen species production is very sensitive to mild uncoupling. Biochem. Soc. Trans. 31, 1300–1301. https://doi.org/10.1042/bst0311300.

Morice, P., Leary, A., Creutzberg, C., Abu-Rustum, N., Darai, E., 2016. Endometrial cancer. Lancet 387, 1094–1108. https://doi.org/10.1016/S0140-6736(15)00130-0.

Mukhtar, E., Adhami, V.M., Mukhtar, H., 2014. Targeting microtubules by natural agents for cancer therapy. Mol. Canc. Therapeut. 13, 275–284. https://doi.org/10.1158/1535-7163.MCT-13-0791.

Muñoz-Espín, D., Serrano, M., 2014. Cellular senescence: from physiology to pathology. Nat. Rev. Mol. Cell Biol. 15, 482–496. https://doi.org/10.1038/nrm3823.

Narita, Masashi, Nuñez, S., Heard, E., Narita, Masako, Lin, A.W., Hearn, S.A., Spector, D. L., Hannon, G.J., Lowe, S.W., 2003. Rb-mediated heterochromatin formation and silencing of E2F target genes during cellular senescence. Cell 113, 703–716. https://doi.org/10.1016/S0092-8674(03)00401-X.

Ouyang, L., Shi, Z., Zhao, S., Wang, F.-T., Zhou, T.-T., Liu, B., Bao, J.-K., 2012. Programmed cell death pathways in cancer: a review of apoptosis, autophagy and programmed necrosis. Cell Prolif 45, 487–498. https://doi.org/10.1111/j.1365-2184.2012.00845.x.

Paglin, S., Hollister, T., Delohery, T., Hackett, N., McMahill, M., Sphicas, E., Domingo, D., Yahalom, J., 2001. A novel response of cancer cells to radiation involves autophagy and formation of acidic vesicles. Canc. Res. 61, 439–444.

Paul, S., Hwang, J.K., Kim, H.Y., Jeon, W.K., Chung, C., Han, J.-S., 2013. Multiple biological properties of macelignan and its pharmacological implications. Arch Pharm. Res. (Seoul) 36, 264–272. https://doi.org/10.1007/s12272-013-0048-z.

Pawlowska, E., Szczepanska, J., Szatkowska, M., Blasiak, J., 2018. An interplay between senescence, apoptosis and autophagy in glioblastoma multiforme—role in pathogenesis and therapeutic perspective. Int. J. Mol. Sci. 19, 889. https://doi.org/10.3390/ijms19030889.

Perillo, B., Di Donato, M., Pezone, A., Di Zazzo, E., Giovannelli, P., Galasso, G., Castoria, G., Migliaccio, A., 2020. ROS in cancer therapy: the bright side of the moon. Exp. Mol. Med. 52, 192–203. https://doi.org/10.1038/s12276-020-0384-2.

Pramod, K., Ansari, S.H., Ali, J., 2010. Eugenol: a natural compound with versatile pharmacological actions. Nat. Prod. Commun. 5 https://doi.org/10.1177/1934578X1000501236, 1934578X1000501.

Raza, H., John, A., 2005. Green tea polyphenol epigallocatechin-3-gallate differentially modulates oxidative stress in PC12 cell compartments. Toxicol. Appl. Pharmacol. 207, 212–220. https://doi.org/10.1016/j.taap.2005.01.004.

Righi, A.A., Alves, T.R., Negri, G., Marques, L.M., Breyer, H., Salatino, A., 2011. Brazilian red propolis: unreported substances, antioxidant and antimicrobial activities. J. Sci. Food Agric. 91, 2363–2370. https://doi.org/10.1002/jsfa.4468.

Roninson, I.B., 2003. Tumor cell senescence in cancer treatment. Canc. Res. 63, 2705–2715.

Schmittgen, T.D., Livak, K.J., 2008. Analyzing real-time PCR data by the comparative CT method. Nat. Protoc. 3, 1101–1108. https://doi.org/10.1038/nprot.2008.73.

Siddiqui, M., Rajkumar, S.V., 2012. The high cost of cancer drugs and what we can do about it. Mayo Clin. Proc. 87, 935–943. https://doi.org/10.1016/j.mayocp.2012.07.007.

Siegel, R.L., Miller, K.D., Jemal, A., 2019. Cancer statistics, 2019. CA. Cancer J. Clin. 69, 7–34. https://doi.org/10.3322/caac.21551.

Sotler, R., Poljšak, B., Dahmane, R., Jukić, T., Pavan Jukić, D., Rotim, C., Trebše, P., Starc, A., 2019. Prooxidant activities of antioxidants and their impact on health. Acta Clin. Croat. 58, 726–736. https://doi.org/10.20471/acc.2019.58.04.20.

Starkov, A.A., Fiskum, G., 2003. Regulation of brain mitochondrial H2O2 production by membrane potential and NAD(P)H redox state. J. Neurochem. 86, 1101–1107. https://doi.org/10.1046/j.1471-4159.2003.01908.x.

Stein, G.H., Drullinger, L.F., Robetorye, R.S., Pereira-Smith, O.M., Smith, J.R., 1991. Senescent cells fail to express cdc2, cycA, and cycB in response to mitogen stimulation. Proc. Natl. Acad. Sci. Unit. States Am. 88, 11012–11016. https://doi.org/10.1073/pnas.88.24.11012.

Strober, W., 2015. Trypan Blue Exclusion Test of Cell Viability. https://doi.org/10.1002/0471142735.ima03bs111. Curr. Protoc. Immunol. 111, A3.B.1-A3.B.3.

Taneja, S.C., Qazi, G.N., 2006. Bioactive Molecules in Medicinal Plants: A Perspective on Their Therapeutic Action. In: Drug Discovery and Development, vol. I. John Wiley and Sons, pp. 1–50. https://doi.org/10.1002/9780470085226.ch1.

Thuong, P.T., Hung, T.M., Khoi, N.M., Nhung, H.T.M., Chinh, N.T., Quy, N.T., Jang, T.S., Na, M., 2014. Cytotoxic and anti-tumor activities of lignans from the seeds of Vietnamese nutmeg Myristica fragrans. Arch Pharm. Res. (Seoul) 37, 399–403. https://doi.org/10.1007/s12272-013-0185-4.

Torti, S.V., Torti, F.M., 2013. Iron and cancer: more ore to be mined. Nat. Rev. Canc. 13, 342–355. https://doi.org/10.1038/nrc3495.

Uehara, T., Mitsuhashi, A., Tsuruoka, N., Shozu, M., 2015. Metformin potentiates the anticancer effects of cisplatin under normoxic conditions in vitro. Oncol. Rep. 33, 744–750. https://doi.org/10.3892/or.2014.3611.

Urick, M.E., Bell, D.W., 2019. Clinical actionability of molecular targets in endometrial cancer. Nat. Rev. Canc. 19, 510–521. https://doi.org/10.1038/s41568-019-0177-x.

Van Gils, C., Cox, P.A., 1994. Ethnobotany of nutmeg in the spice islands. J. Ethnopharmacol. 42, 117–124. https://doi.org/10.1016/0378-8741(94)90105-8.

Wang, X., Roper, M.G., 2014. Measurement of DCF fluorescence as a measure of reactive oxygen species in murine islets of Langerhans. Anal. Methods 6, 3019–3024. https://doi.org/10.1039/C4AY00288A.

WHO, 2018. World health organization fact sheets: cancer 2018 [WWW document]. 12 sept. URL. https://www.who.int/news-room/fact-sheets/detail/cancer.

Yim, W.W.-Y., Mizushima, N., 2020. Lysosome biology in autophagy. Cell Discov. 6, 6. https://doi.org/10.1038/s41421-020-0141-7.

Yoo, C.-B., Han, K.-T., Cho, K.-S., Ha, J., Park, H.-J., Nam, J.-H., Kil, U.-H., Lee, K.-T., 2005. Eugenol isolated from the essential oil of Eugenia caryophyllata induces a reactive oxygen species-mediated apoptosis in HL-60 human promyelocytic leukemia cells. Canc. Lett. 225, 41–52. https://doi.org/10.1016/j.canlet.2004.11.018.

Young, A.R.J., Narita, M., Ferreira, M., Kirschner, K., Sadaie, M., Darot, J.F.J., Tavare, S., Arakawa, S., Shimizu, S., Watt, F.M., Narita, M., 2009. Autophagy mediates the mitotic senescence transition. Genes Dev. 23, 798–803. https://doi.org/10.1101/gad.519709.

Zhang, Y.-J., Gan, R.-Y., Li, S., Zhou, Y., Li, A.-N., Xu, D.-P., Li, H.-B., 2015. Antioxidant phytochemicals for the prevention and treatment of chronic diseases. Molecules 20, 21138–21156. https://doi.org/10.3390/molecules201219753.

Zorova, L.D., Popkov, V.A., Plotnikov, E.Y., Silachev, D.N., Pevzner, I.B., Jankauskas, S. S., Babenko, V.A., Zorov, S.D., Balakireva, A.V., Juhaszova, M., Sollott, S.J., Zorov, D.B., 2018. Mitochondrial membrane potential. Anal. Biochem. 552, 50–59. https://doi.org/10.1016/j.ab.2017.07.009.